An extended state observer with adjustable bandwidth for measurement noise

ZHANG Shihua[*], QI Xiaohui, and YANG Sen

Shijiazhuang Campus, Army Engineering University of PLA, Shijiazhuang 050053, China

Abstract: In this paper, a bandwidth-adjustable extended state observer (ABESO) is proposed for the systems with measurement noise. It is known that increasing the bandwidth of the observer improves the tracking speed but tolerates noise, which conflicts with observation accuracy. Therefore, we introduce a bandwidth scaling factor such that ABESO is formulated to a 2-degree-of-freedom system. The observer gain is determined and the bandwidth scaling factor adjusts the bandwidth according to the tracking error. When the tracking error decreases, the bandwidth decreases to suppress the noise, otherwise the bandwidth does not change. It is proven that the error dynamics are bounded and converge in finite time. The relationship between the upper bound of the estimation error and the scaling factor is given. When the scaling factor is less than 1, the ABESO has higher estimation accuracy than the linear extended state observer (LESO). Simulations of an uncertain nonlinear system with compound disturbances show that the proposed ABESO can successfully estimate the total disturbance in noisy environments. The mean error of total disturbance of ABESO is 15.28% lower than that of LESO.

Keywords: extended state observer (ESO), boundedness and convergence, adjustable bandwidth, measurement noise.

1. Introduction

Uncertainties and disturbances are unavoidable phenomena in industrial control systems, and they adversely affect the quality of their control. A common strategy for estimating system uncertainties and external disturbances is to use an extended state observer (ESO) [1], which takes as input the control signals and measurable information of the system, and outputs the estimated total disturbance of the system and unmeasured state variables. In this way, an uncertain system can be controlled using simultaneous disturbance estimation and feedforward dis-

turbance compensation strategies. An ESO-based control scheme is an attractive solution because it can deal with disturbances in uncertain systems directly and in time. To date, it has been successfully applied in a variety of fields and resolved numerous control problems [2−4]. The theoretical research and verification of ESO has also achieved remarkable results [5−7].

In the actual engineering control system, high frequency noise is inevitably introduced when the output is measured, including spacecraft attitude control [8], unmanned ground vehicles [9], electronic throttle system [5]. If high frequency noise can pass through the ESO, it will contaminate the estimates. Then, controllers utilizing such estimates contain redundant parts associated with amplifying noise. Not only do these parts increase energy usage to saturate the control input, but high-frequency components retained in the control input excite the high-frequency unmodeled dynamics of the system, which can reduce the control performance and even destroy closed-loop stability [5]. However, in the design of ESOs, the gain of the observer will be increased in order to improve the tracking speed, and the noise will be amplified at the same time, so that adverse effects caused by measurement noise cannot be ignored. Therefore, designing ESOs for systems with measurement noise has always been an attractive research topic.

So far, scholars have proposed many solutions to attenuate measurement noise, which can be divided into two distinct approaches. The first approach is to modify the observer design, mainly including: combining ESO with a Kalman filter [5,10], cascading observers [6,7], designing linear and nonlinear parts without any switching elements [9]. In the other approach, gain adjustment techniques are used to improve estimation accuracy and noise immunity. In [11], the gain adaptation was implemented as the output of a stable filter using the squared norm of the measured output estimation error and the mismatch between each estimate and its saturated value. Ahrens et

al. [12] proposed a technique by which the gain matrix of a high gain observer was switched between two values. Its purpose was to take advantage of higher gain during transients, providing better estimation and tracking. Once the tracking error arrived at the threshold, the gain was switched to a smaller value to suppress measurement noise. However, in order to avoid repeated switching, it is necessary to ensure the monotonic decrease of the estimation error and consider the influence of the initial peak value, which increases the difficulty complexity of numerical implementation. In [13], a bi-bandwidth ESO (BESO) was proposed using the switching technique. The gain switching is triggered by the transient variation tendency of the estimation error, and no additional threshold is required to determine the switching zone. However, only the convergence of second-order BESO was studied in [13]. Although this approach was extended to multiple-input-multiple-output (MIMO) systems, the observer remains essentially a second-order BESO since the observed plant is fully measurable. The difficulty of designing BESO with order higher than 2 is to prove the stability of switching system. In addition, since the gain is switched repeatedly between two values, if the two values differ greatly, the bandwidth adjustment will be too large, resulting in the observer being more sensitive to the bounded noise.

Inspired by [13], a switched-gain technique is employed to the extended state observer. We use the change rate of absolute value of estimation error to define a bandwidth scaling factor. If the error increases, a larger bandwidth is needed to improve the tracking speed. However, in order to prevent the bandwidth adjustment from being too large, the bandwidth is kept unchanged at this time. If the error is reduced, a smaller bandwidth is needed to suppress the noise. Thus, the bandwidth is reduced compared to the original one. In this way, a 2-degree-of-freedom observer is obtained. By designing appropriate gain and bandwidth scaling factor, both tracking speed and noise suppression are taken into account. In addition, we give a sufficient condition for the stability of the third-order switching system. It is proved that the proposed ESO in this paper is convergent and the relation between the upper bound of the estimation error and the bandwidth scaling factor is given. Theoretical analysis shows that when the scaling factor is less than 1, the ABESO proposed in this paper has higher estimation accuracy than LESO.

The contents and organization outlines are as follows: Section 2 introduces the statement of the problem. Section 3 presents the convergence analysis of ABESO. Section 4 performs the numerical simulations to compare effects of LESO, BESO, and ABESO on the noise sup-

pression. Section 5 summarizes the main work of this paper.

2. Problem statement

A general second order nonlinear uncertain system is considered:

$$
\begin{cases}
\ddot{x}(t) = a\dot{x}(t) + b^*(x(t) + g(x)u(t) + f(x) + d^*(t)) \\
y(t) = x(t) + \omega(t)
\end{cases}
$$

where $a, b^* \in \mathbf{R}$ are constants, $\dot{x}(t)$ and $\ddot{x}(t)$ denote the first derivative and second derivative of $x(t)$, respectively, $u(t) \in \mathbf{R}$ is the control input, $d^*(t) \in \mathbf{R}$ is the unknown external disturbance, $g(x) \in \mathbf{R}$ represents the influence of the control signal on the system dynamics, $f(x) \in \mathbf{R}$ describes nonlinear internal dynamics, $y(t) \in \mathbf{R}$ is the system output, and $\omega(t) \in \mathbf{R}$ corresponds to high frequency noise. Such systems often appear in electromechanical and mechanical systems, where position is measured.

Let $\hat{g} \in \mathbf{R} \backslash \{0\}$ be a nominal value of $g(x)$. The system can be written as

$$
\begin{cases}
\ddot{x}(t) = bu(t) + d(t, x) \\
y(t) = x(t) + \omega(t)
\end{cases},
\tag{1}
$$

where $b = b^*\hat{g}$, and

$$
d(t, x) = a\dot{x}(t) + b^*(x(t) + f(x)) + \\
b^*((g(x) - \hat{g})u(t) + d^*(t))
$$

is defined as the total disturbance depending on the state of the system and external disturbances, including the effects of external disturbances, model parameter perturbations, nonlinearity of the system, etc.

The state-space model of system in (1) is represented as follow:

$$
\begin{cases}
\dot{x}_1(t) = x_2(t) \\
\dot{x}_2(t) = d(t, x) + bu(t) \\
y(t) = x_1(t) + \omega(t)
\end{cases}.
\tag{2}
$$

Obviously, system in (2) is observable. This paper focuses on the disturbance observation problem. Thus, we can give the following assumption.

Assumption 1 The system in (1) is stable or the closed loop is stable, which implies $x(t)$ and its derivative are bounded. The derivative of the total disturbance $d(t, x)$ is also bounded as

$$
|\dot{d}(t, x)| \leqslant m_d.
$$

This assumption represents a class of continuous time-varying disturbances, such as slow and fast disturbances that exist in many practical applications.

Assumption 2 Assume that the measurement noise $\omega(t)$ is bounded, i.e.,

$$|\omega(t)| \leqslant m_\omega.$$

Since the traditional LESO only takes the bandwidth as an adjustable parameter, it cannot take into account the measurement noise and estimation accuracy at the same time. Ahrens et al. [12] proposed a "switching zone" to adjust the bandwidth, considering that transient and steady-state responses had different requirements for observer gain. But there is no good way to determine the switching threshold. Then, Prasov et al. [14] proposed a scheme to adjust the threshold, however, it would increase the burden and uncertainty of implementation. In [13], a directional switching operator was defined to make the gain switch between two values without threshold. However, the extended state observer was only for the first-order plant. Even if generalized to MIMO systems, it was essentially a second-order ESO that reconstructed the state and disturbance of a specified type of system. Inspired by [12−14], for system in (1), an ABESO is designed as

$$\begin{cases} \dot{\hat{x}}_1(t) = \hat{x}_2(t) + l_1\delta e_n(t) \\ \dot{\hat{x}}_2(t) = \hat{x}_3(t) + bu(t) + l_2\delta^2 e_n(t) \,, \\ \dot{\hat{x}}_3(t) = l_3\delta^3 e_n(t) \end{cases} \tag{3}$$

where

$$\delta = \rho^{-\min\left\{\text{sign}\left(\frac{d|e_n(t)|}{dt}\right),0\right\}}. \tag{4}$$

In the ABESO, $\hat{x}_i(t)(i = 1, 2, 3)$ are the states of the observer, $e_n = \hat{x}_1(t) - y(t)$ is the estimation error of $y(t)$, including measurement noise, $l_i(i = 1, 2, 3)$ are observer gains, δ is defined as a bandwidth scaling factor, in which $\rho > 0$ is a constant, the value range will be determined later.

Obviously, (3) is a LESO if $\rho = 1$. The observer gains can be chosen as

$$\begin{cases} l_1 = -3w_o \\ l_2 = -3w_o^2 \\ l_3 = -w_o^3 \end{cases} \tag{5}$$

via the parameter tuning technique in [15]. Here, $w_o > 0$ represents the bandwidth of the observer. Following this approach, all three poles are placed at w_o. If $\rho \neq 1$, the parameter δ switches between 1 and ρ, adjusting the bandwidth of the observer according to the direction of the tracking error.

Remark 1 The estimation performances of ABESO are better when the parameter $\rho < 1$. If the absolute value of estimation error decreases, $\delta = \rho$, the bandwidth of the observer is $w_o\rho$ which becomes smaller to suppress the noise. Otherwise, $\delta = 1$, the bandwidth is w_o, which provides fast tracking speed. In [13], the observer bandwidth

switched between $w_o\rho$ and w_o/ρ. Large and frequent switching of bandwidth increases estimation error. Subsequent theoretical analysis and numerical simulations show that our gain adjustment strategy outperforms the one proposed in [13].

3. Convergence of ABESO

In this section, we will study the convergence of the proposed ABESO. Select the same observer gains as (5) in the following paper.

Define

$$\begin{cases} e_i(t) = \hat{x}_i(t) - x_i(t), \quad i = 1, 2, 3 \\ e(t) = (e_1(t), e_2(t), e_3(t))^T \end{cases}.$$

The error dynamic system for system (1) and (3) is as follows:

$$\dot{e}(t) = A_\delta e(t) + H_\delta(t) \tag{6}$$

where

$$A_\delta = \begin{pmatrix} -3w_o\delta & 1 & 0 \\ -3w_o^2\delta^2 & 0 & 1 \\ -w_o^3\delta^3 & 0 & 0 \end{pmatrix},$$

$$H_\delta(t) = \begin{pmatrix} 3w_o\delta\omega(t) \\ 3w_o^2\delta^2\omega(t) \\ w_o^3\delta^3\omega(t) - \dot{d}(t,x) \end{pmatrix}. \tag{7}$$

Due to the definition of δ, A_δ has the following two forms:

$$A_1 = \begin{pmatrix} -3w_o\rho & 1 & 0 \\ -3w_o^2\rho^2 & 0 & 1 \\ -w_o^3\rho^3 & 0 & 0 \end{pmatrix},$$

$$A_2 = \begin{pmatrix} -3w_o & 1 & 0 \\ -3w_o^2 & 0 & 1 \\ -w_o^3 & 0 & 0 \end{pmatrix},$$

where $\rho > 0, \rho \neq 1$. Therefore, the system in (6) is a switched linear system consisting of two modes. Firstly, the stability of the switched linear system

$$\dot{e}(t) = A_\delta e(t) \tag{8}$$

is investigated, whose subsystems are linear time-invariant systems

$$\dot{e}(t) = A_i e(t), \quad i = 1, 2.$$

Lemma 1 [16] Let A_1, A_2 be two Hurwitz matrices in $\mathbf{R}^n$ with rank$(A_1 - A_2) = 1$. A necessary and sufficient condition for the existence of a common quadratic Lyapunov function for the switched system in (8) with A_1, A_2 as the two subsystems is that the matrix product A_2A_1 does not have any negative real eigenvalues.

All subsystems of the switched system have a common quadratic Lyapunov function to guarantee the

quadratic stability of the switched system. Quadratic stability means asymptotic stability , which is a special kind of exponential stability. Based on Lemma 1, the stability of the system in (8) is shown below.

Lemma 2   If $w_o > 0, \rho > 0$, the system in (8) is quadratically stable.

Proof   Let γ be the eigenvalue of matrix $\boldsymbol{A}_\delta$. The characteristic equation of matrix $\boldsymbol{A}_\delta$ is

$$\gamma^3 + 3w_o\delta\gamma^2 + 3w_o^2\delta^2\gamma + w_o^3\delta^3 = 0.$$

Using the Routh-Hurwitz stability criterion, $\boldsymbol{A}_\delta$ is a Hurwitz matrix if and only if $w_o > 0, \delta > 0$. Furthermore, we have

$$\mathrm{rank}(\boldsymbol{A}_1 - \boldsymbol{A}_2) = \mathrm{rank}\begin{pmatrix} -3w_o\rho + 3w_o & 0 & 0 \\ -3w_o^2\rho^2 + 3w_o^2 & 0 & 0 \\ -w_o^3\rho^3 + w_o^3 & 0 & 0 \end{pmatrix} = 1.$$

Below we will discuss the eigenvalues of $\boldsymbol{A}_2\boldsymbol{A}_1$. Calculate the matrix product:

$$\lambda^3 + 3w_o^2(\rho^2 - 3\rho + 1)\lambda^2 - 3w_o^4\rho(\rho^2 - 3\rho + 1)\lambda - w_o^6\rho^3 = 0. \tag{9}$$

Denote

$$p = \rho^2 - 3\rho + 1,$$
$$F(\lambda) = \lambda^3 + 3w_o^2 p\lambda^2 - 3w_o^4\rho p\lambda - w_o^6\rho^3.$$

Obviously,

$$\begin{cases} \lim_{\lambda\to+\infty} F(\lambda) = +\infty \\ \lim_{\lambda\to-\infty} F(\lambda) = -\infty \end{cases}. \tag{10}$$

Calculating the derivative of $F(\lambda)$, we have

$$F'(\lambda) = 3\lambda^2 + 6w_o^2 p\lambda - 3w_o^4\rho p.$$

Let

$$\Delta = 36w_o^4 p(p + \rho).$$

According to the definition of p, we have

$$p + \rho = (\rho - 1)^2 \geqslant 0.$$

In the following, we discuss three cases.

(i) $\Delta < 0$, that is $p < 0$. $F'(\lambda)$ has no zero point, which means $F'(\lambda) > 0$ when $\lambda \in \mathbf{R}$. Therefore, $F(\lambda)$ is a monotonically increasing function. Under the condition (10), the characteristic equation (9) has a unique real root. In addition,

$$F(0) = -w_o^6\rho^3 < 0,$$

which indicates that the unique real root is positive.

(ii) $\Delta = 0$. This case is similar to the first case, the characteristic equation has only one positive real root.

(iii) $\Delta > 0$, that is $p > 0$. In this case, $F'(\lambda)$ has two zero points, i.e.,

$$\underline{\lambda} = w_o^2\left(-p - \sqrt{p(p+\rho)}\right) < 0 < w_o^2\left(-p + \sqrt{p(p+\rho)}\right) = \overline{\lambda},$$

which are also the two extreme points of $F(\lambda)$. Since the quadratic curve of the function $F'(\lambda)$ opens upward, the function $F(\lambda)$ must first increase, then decrease, then increase. Note that

$$\lambda_1\lambda_2\lambda_3 = w_o^6\rho^3 > 0$$

where $\lambda_i(i = 1, 2, 3)$ are the three roots of $F(\lambda) = 0$. Therefore, the characteristic equation (9) has at least one positive real root, written as $\lambda_1 > 0$. Whether the characteristic equation has negative real roots can be discussed by analyzing the extreme points $\underline{\lambda}$ and $\overline{\lambda}$. From the above analyses, $\underline{\lambda}, \overline{\lambda}$ are the maximum and minimum points of $F(\lambda)$, respectively. Therefore, $F(\lambda)$ does not have any negative zero points if and only if $F(\underline{\lambda}) < 0$. By calculation, we have

$$F(\underline{\lambda}) = w_o^6\left(-p - \sqrt{p(p+\rho)}\right)^3 + 3w_o^6 p\left(-p - \sqrt{p(p+\rho)}\right)^2 -$$
$$3w_o^6\rho p\left(-p - \sqrt{p(p+\rho)}\right) - w_o^6\rho^3 =$$
$$-w_o^6\left(p + \sqrt{p(p+\rho)} + \rho\right)\left[\left(-p - \sqrt{p(p+\rho)}\right)^2 +\right.$$
$$\left.\rho\left(p + \sqrt{p(p+\rho)}\right) + 3p\right].$$

Obviously, $F(\underline{\lambda}) < 0$. In conclusion, the matrix $\boldsymbol{A}_2\boldsymbol{A}_1$ does not have any negative eigenvalues. $\square$

Above we have shown the stability of the switched linear system in (8), i.e., all subsystems have a common quadratic Lyapunov function. Below we analyze the derivative of the Lyapunov function along (6) to obtain the convergence of $\|\boldsymbol{e}(t)\|$.

Theorem 1   The estimation error $\|\boldsymbol{e}(t)\|$ will ultimately converge to a bound in finite time.

Proof   Changing variables as $\boldsymbol{e} = \boldsymbol{\Lambda}\boldsymbol{\eta}$, where $\boldsymbol{\Lambda} = \mathrm{diag}\{w_o^{-2}, w_o^{-1}, 1\},\ \boldsymbol{\eta} \in \mathbf{R}^3$, (6) can be transformed into

$$\dot{\boldsymbol{\eta}}(t) = w_o\boldsymbol{A}'_\delta\boldsymbol{\eta}(t) + \boldsymbol{H}'_\delta(t), \tag{11}$$

where

$$\boldsymbol{A}'_\delta = \begin{pmatrix} -3\delta & 1 & 0 \\ -3\delta^2 & 0 & 1 \\ -\delta^3 & 0 & 0 \end{pmatrix},$$

$$\boldsymbol{H}'_\delta(t) = \begin{pmatrix} 3w_o^3\delta\omega(t) \\ 3w_o^3\delta^2\omega(t) \\ w_o^3\delta^3\omega(t) - \dot{d}(t, x) \end{pmatrix}.$$

Since $\boldsymbol{A}'_\delta$ is a special case of $\boldsymbol{A}_\delta$ when $w_o = 1$, it can be seen from Lemma 2 that there is a positive definite symmetric matrix $\boldsymbol{P} \in \mathbf{R}^{3\times3}$, satisfying

$$\boldsymbol{A}'^{\mathrm{T}}_\delta\boldsymbol{P} + \boldsymbol{P}\boldsymbol{A}_\delta = -\boldsymbol{I}$$

where $\boldsymbol{I}$ is an identity matrix. Note that $\boldsymbol{P}$ is a matrix determined by δ, and independent of w_o. Define a Lyapunov function

$$V(\boldsymbol{\eta}) = \frac{1}{2}\boldsymbol{\eta}^{\mathrm{T}}(t)P\boldsymbol{\eta}(t),$$

which satisfies

$$\lambda_{\min}(\boldsymbol{P})\|\boldsymbol{\eta}(t)\|^2 \leqslant V(\boldsymbol{\eta}) \leqslant \lambda_{\max}(\boldsymbol{P})\|\boldsymbol{\eta}(t)\|^2 \qquad (12)$$

where $\lambda_{\min}(\boldsymbol{P})$ and $\lambda_{\max}(\boldsymbol{P})$ are the minimum and maximum eigenvalues of $\boldsymbol{P}$, respectively, $\|\cdot\|$ represents the 2-norm in this paper. Compute the derivative of $V(\boldsymbol{\eta})$ with respect to time t along (11), giving

$$\dot{V}(\boldsymbol{\eta}) = w_o\boldsymbol{\eta}^{\mathrm{T}}(t)(A_\delta^{'\mathrm{T}}\boldsymbol{P} + \boldsymbol{P}A_\delta)\boldsymbol{\eta}(t) + 2\boldsymbol{\eta}^{\mathrm{T}}(t)\boldsymbol{P}H_\delta^{'\mathrm{T}}(t) \leqslant$$
$$- w_o\|\boldsymbol{\eta}(t)\|^2 + 2\lambda_{\max}(\boldsymbol{P})\|\boldsymbol{\eta}(t)\|\|\boldsymbol{H}'_\delta(t)\| \leqslant$$
$$- w_o\|\boldsymbol{\eta}(t)\|^2 + 2\lambda_{\max}(\boldsymbol{P})\|\boldsymbol{\eta}(t)\|(w_o^3\bar{\delta}m_\omega + m_d) \qquad (13)$$

where $\bar{\delta} = 9\delta^2 + 9\delta^4 + \delta^6$. From (12), we can get that

$$\frac{1}{\lambda_{\max}(\boldsymbol{P})}V(\boldsymbol{\eta}) \leqslant \|\boldsymbol{\eta}(t)\|^2 \leqslant \frac{1}{\lambda_{\min}(\boldsymbol{P})}V(\boldsymbol{\eta}). \qquad (14)$$

Let

$$L = \frac{4\lambda_{\max}^4(\boldsymbol{P})}{\mu^2\lambda_{\min}(\boldsymbol{P})}\left(w_o^2\bar{\delta}m_\omega + \frac{m_d}{w_o}\right)^2 \qquad (15)$$

where $\mu \in (0, 1)$ is a constant. Since $V(\boldsymbol{\eta})$ is positive definite, if $V(\boldsymbol{\eta}) \geqslant L$, then

$$V^{\frac{1}{2}}(\boldsymbol{\eta}) \geqslant \frac{2\lambda_{\max}^2(\boldsymbol{P})}{\mu\lambda_{\min}^{\frac{1}{2}}(\boldsymbol{P})}\left(w_o^2\bar{\delta}m_\omega + \frac{m_d}{w_o}\right). \qquad (16)$$

Combining (14) and (16), we derive that

$$V(\boldsymbol{\eta}) \geqslant \frac{2\lambda_{\max}^2(\boldsymbol{P})}{\mu\lambda_{\min}^{\frac{1}{2}}(\boldsymbol{P})}\left(w_o^2\bar{\delta}m_\omega + \frac{m_d}{w_o}\right)V^{\frac{1}{2}}(\boldsymbol{\eta}) =$$

$$\frac{2\lambda_{\max}^2(\boldsymbol{P})}{\mu}\left(w_o^2\bar{\delta}m_\omega + \frac{m_d}{w_o}\right)\left(\frac{1}{\lambda_{\min}(\boldsymbol{P})}V(\boldsymbol{\eta})\right)^{\frac{1}{2}} \geqslant$$

$$\frac{2\lambda_{\max}^2(\boldsymbol{P})}{\mu}\left(w_o^2\bar{\delta}m_\omega + \frac{m_d}{w_o}\right)\|\boldsymbol{\eta}(t)\|. \qquad (17)$$

Thus, from (13), (14), and (17), if $V(\boldsymbol{\eta}) \geqslant L$, it can be concluded that

$$\dot{V}(\boldsymbol{\eta}) \leqslant -\frac{w_o}{\lambda_{\max}(P)}V(\boldsymbol{\eta}) + \frac{w_o\mu}{\lambda_{\max}(P)}V(\boldsymbol{\eta}) \leqslant$$
$$-\frac{w_o(1-\mu)}{\lambda_{\max}(P)}V(\boldsymbol{\eta}). \qquad (18)$$

Denote

$$D = \{\boldsymbol{\eta}|V(\boldsymbol{\eta}) < L\}. \qquad (19)$$

The inequality (18) shows that any $\boldsymbol{\eta} \notin D$ will converge to D after some time T, satisfying

$$T \leqslant T_0 = \frac{\lambda_{\max}(\boldsymbol{P})}{w_o(1-\mu)}\ln\frac{V_0}{L}, \qquad (20)$$

in which $V_0 = V(\boldsymbol{\eta}(0))$ is the initial value of $V(\boldsymbol{\eta})$. T_0 can be obtained by the comparison theorem.

Note that $\boldsymbol{e} = \Lambda\boldsymbol{\eta}$, therefore, if $t > T_0$, from (15) and (19), we can get that

$$\|\boldsymbol{e}(t)\| \leqslant \|\boldsymbol{\eta}\| \leqslant \sqrt{\frac{V(\boldsymbol{\eta})}{\lambda_{\min}(\boldsymbol{P})}} \leqslant \frac{2\lambda_{\max}^2(\boldsymbol{P})}{\mu\lambda_{\min}(\boldsymbol{P})}\left(w_o^2\bar{\delta}m_\omega + \frac{m_d}{w_o}\right). \quad (21)$$

$\square$

Remark 2 From (21), it can be seen that if there is no measurement noise, i.e., $m_\omega = 0$, the estimation error is determined by the bound on the derivative of the total disturbance. And the slower the total disturbance changes, the smaller the estimation error. In particular, the ABESO converges asymptotically when $m_d = 0$. The disturbance rejection performance of the observer can be improved by increasing the bandwidth. When there is measurement noise in the system, the estimation error is affected by the measurement noise and total disturbance. In this case, a large w_o is beneficial to suppress the total disturbance, but it magnifies the noise. Therefore, a compromise is needed to improve the disturbance rejection performance, which is similar to LESO. However, if $\rho < 1$, from (4) we can get $\bar{\delta} < 1$. In particular, if $\delta = 1$, (21) gives the error bound for LESO. This shows that for systems with measurement noise, the ABESO proposed in this paper has higher estimation accuracy for state and disturbance estimation.

4. Numerical simulations

This section presents a simulation example, defines five performance indicators, and analyzes the disturbance immunity performance of ABESO in transient response and steady-state response. The results are compared with LESO [15] and BESO [13].

For this purpose, a second-order plant is considered:

$$\begin{cases} \ddot{x}(t) = \dfrac{\sin(x_1(t)) + \sin(x_2(t))}{4\pi} + d^*(t) + u(t) \\ y(t) = x(t) + \omega(t) \end{cases} \qquad (22)$$

where $d^*(t)$ is the external disturbance, $\omega(t)$ is the measurement noise. Let

$$d(t, x) = \frac{\sin(x_1(t)) + \sin(x_2(t))}{4\pi} + d^*(t)$$

be the total disturbance. The control objective is to make the output $y(t)$ track the desired trajectory $r(t)$ in the presence of total disturbance $d(t, x)$ and measurement noise $\omega(t)$.

In simulations, we take $d^*(t)$ as the compound disturbance:

$$d^*(t) = \frac{t}{4\pi} + \sin(0.4t + 1).$$

The measurement noise $\omega(t)$ is a Gaussian white noise, whose variance is 0.001. The desired trajectory $r(t)$ and total disturbance $d(t, x)$ are shown in Fig. 1.
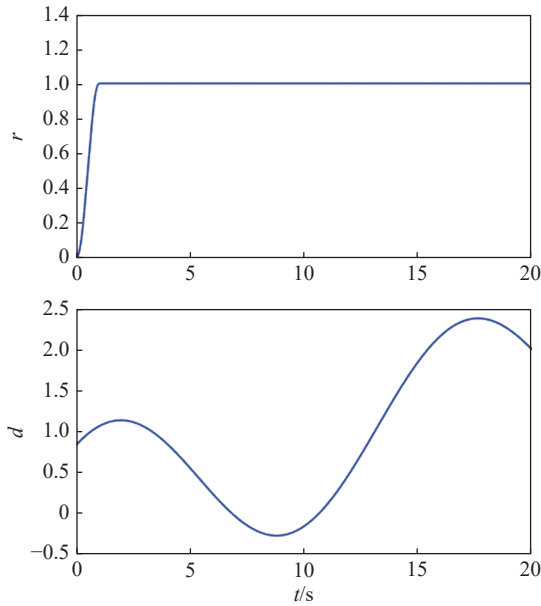
Fig. 1 The desired trajectory $r(t)$ and total disturbance $d(t,x)$

All the simulations are performed using the same outer loop controller and initial states. The outer loop controller is a linear control law:

$$u(t) = \frac{u_0(t) - \hat{x}_3(t)}{b_0},$$

$$u_0(t) = k_p(r(t) - \hat{x}_1(t)) + k_d\hat{x}_2(t),$$

where k_p, k_d are controller parameters, being 25 and -10, respectively. The initial states of the plant (22) and the ESOs are (1, 1) and (0, 0, 0), respectively.

In order to establish a fair base for further comparison, we first define three indicators in Table 1, which respectively represent the mean error of state x and $\dot{x}$ and the total disturbance $d(t,x)$. Many numerical experiments are carried out on the design parameters to determine the optimal indicator. Then, we define another two indicators: rise time t_r and error peak $|e_{\max}|$, which represent the time when the error converges to $[-0.01, 0.01]$ and the maximum deviation of response, respectively.

Table 1 Mean error indexes

Index	Expression
J_{e_x}	$\frac{1}{t}\int_0^t |x(s) - \hat{x}(s)|\mathrm{d}s$
$J_{e_{\dot{x}}}$	$\frac{1}{t}\int_0^t |\dot{x}(s) - \hat{\dot{x}}(s)|\mathrm{d}s$
J_{e_d}	$\frac{1}{t}\int_0^t |d(s) - \hat{d}(s)|\mathrm{d}s$

Example 1 Performances of LESO. Taking $\rho = 1$ and $l_i(i = 1, 2, 3)$ as (5), system in (3) is the LESO designed in (16). There is only one tunable parameter w_o. Let w_o change from 4 to 10, and Table 2 lists the mean error indexes. It can be seen from Table 2 that the index J_{e_x} first decreases and then increases as w_o changes from

4 to 10. However, the indexes J_{e_x} and J_{e_d} keep increasing. This means that for $w_o = 5, 6, 7$, the estimation performances of LESO are better in the mean error sense. Therefore, we take $w_o = 5, 6, 7$ to further analyze the disturbance rejection performance of LESO in transient response and steady-state response. Fig. 2 shows the estimation errors for the three bandwidths, and the fourth plot is the trajectory of total disturbance by LESO when $w_o = 7$. The first three plots locally amplify the transient and steady-state responses, respectively. Their rise times and error peaks are listed in Table 3. As shown in Fig. 2 and Table 3, the rise time becomes shorter and the peak error becomes larger with the increase of bandwidth.

Table 2 LESO mean error indexes with the bandwidth changing from 4 to 10

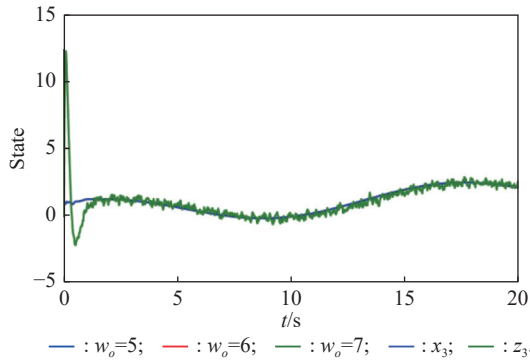| Index	w_o						
	4	5	6	7	8	9	10
J_{e_x}	1.76	1.68	1.65	1.66	1.72	1.74	1.77
$J_{e_{\dot{x}}}$	10.79	10.73	11.53	12.75	14.85	16.83	17.21
J_{e_d}	26.03	26.32	28.73	33.48	40.43	48.91	59.03
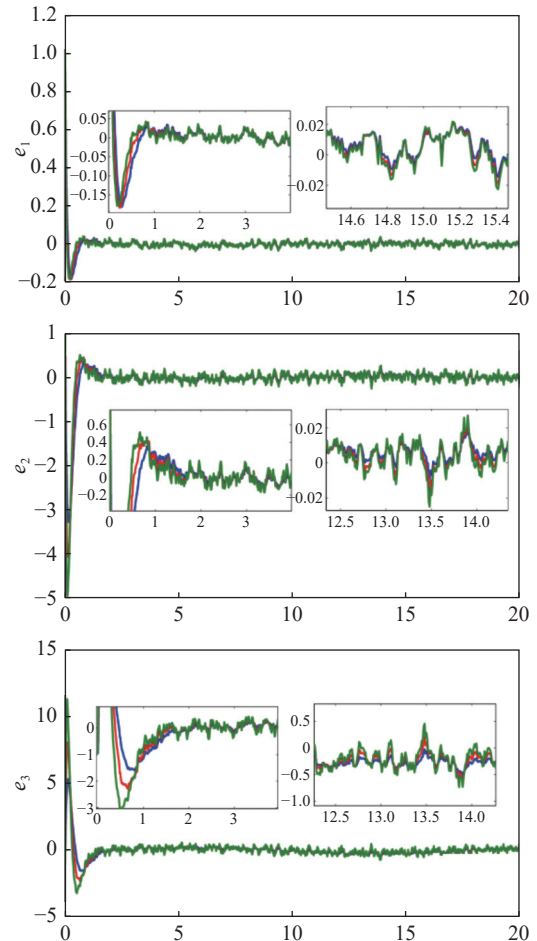
Fig. 2   LESO performances in estimating compound disturbances with measurement noise

Table 3   Rise time and peakings of LESO for bandwidth changing from 5 to 7

Index	w_o								
	5			6			7		
e_i	e_x	$e_{\dot{x}}$	e_d	e_x	$e_{\dot{x}}$	e_d	e_x	$e_{\dot{x}}$	e_d
t_r	0.7	0.64	2.09	0.62	0.52	1.56	0.5	0.46	1.34
$|e_{\max}|$	0.04	0.39	0.53	0.04	0.43	0.62	0.05	0.51	0.73

Example 2   Performances of BESO. The BESO in [13] has two tunable parameters: the bandwidth w_o and ρ. Here we choose $\rho = 0.7$. Still let w_o change from 4 to 10, the indexes of BESO estimation effect are listed in Table 4. The mean error indicator J_{e_x} is not strictly first-increasing and then decreasing. But considering these three indicators, when $w_o = 5, 6, 7$, the estimation effect of BESO is better. Table 5 and Fig. 3 show the detailed estimation errors of BESO. From Table 5, we see that the rise time t_r decreases as w_o increases, but $|e_{\max}|$ increases. Compared to LESO, the rise times of e_x and $e_{\dot{x}}$ are shorter when observed with BESO. However, since the gain switches widely, BESO is more sensitive to the measurement noise. Especially for total disturbance, as shown in the fourth plot of Fig. 3, $\hat{x}_3$ does not track $d(t, x)$ very well. The gain of ABESO switches between 1 and ρ, which improves the disturbance rejection performance and is demonstrated in the example below.

Table 4   BESO mean error indexes with the bandwidth changing from 4 to 10

Index	w_o						
	4	5	6	7	8	9	10
J_{e_x}	2.84	2.76	2.68	2.59	2.78	2.66	2.77
$J_{e_{\dot{x}}}$	19.91	23.34	25.85	27.97	34.49	35.36	39.93
J_{e_d}	39.10	53.34	70.59	89.23	119.52	142.82	171.19

Table 5   Rise time and peakings of BESO for bandwidth changing from 5 to 7

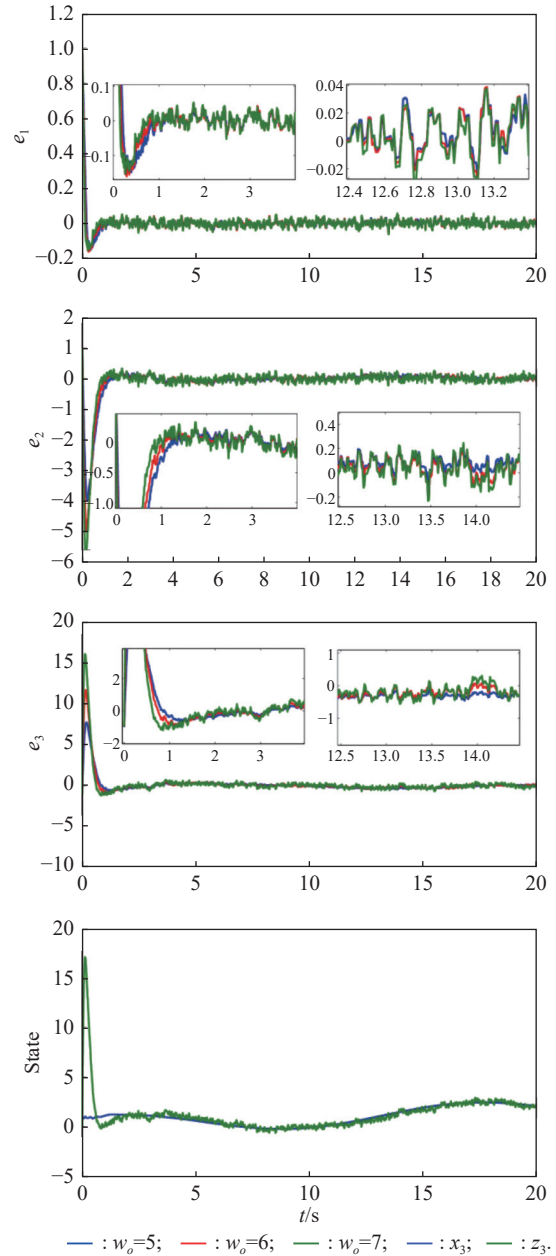| Index	w_o								
	5			6			7		
e_i	e_x	$e_{\dot{x}}$	e_d	e_x	$e_{\dot{x}}$	e_d	e_x	$e_{\dot{x}}$	e_d
t_r	0.64	0.57	2.22	0.51	0.47	2.22	0.47	0.39	2.22
$|e_{\max}|$	0.06	0.61	0.94	0.06	0.71	1.26	0.06	0.97	1.64

Fig. 3   BESO performances in estimating compound disturbances with measurement noise

Example 3   Performances of ABESO. There are two tunable parameters that are identical to BESO and take the same value. Table 6 and Table 7 are the ABESO

indexes and estimation errors, respectively. The detailed estimation performances when $w_o = 5, 6, 7$ are shown in Fig. 4. When w_o changes from 4 to 9, three estimation indexes for ABESO are the smallest among the three ESOs. Table 8 lists the comparisons of ABESO with LESO and BESO. In Table 8, Reduction[1] represents the reduction rate of ABESO relative to LESO, and Reduction[2] represents the reduction rate of ABESO relative to BESO. Note that for the index J_{e_d}, the reduction rates of ABESO relative to LESO and BESO are 15.28% and 68.21%, respectively. Hence, the ABESO proposed in this paper has higher estimation accuracy for total disturbance. As shown in the fourth plot of Fig. 4, the total disturbance $d(t, x)$ of the plant in (22) is well tracked, in the presence of measurement noise. Furthermore, the rise time of ABESO is faster than that of LESO, and the ABESO tracks total disturbance faster than the BESO. This means that in the presence of measurement noise, ABESO can quickly track system states and disturbances, improving observation performance. However, it is also noted that ABESO has no obvious effect on peaking.

Table 6 ABESO mean error indexes with the bandwidth changing from 4 to 10

Index	w_o						
	4	5	6	7	8	9	10
J_{e_x}	1.57	1.50	1.54	1.57	1.67	1.72	1.87
$J_{e_{\dot{x}}}$	8.97	8.81	10.10	11.03	14.13	15.63	21.54
J_{e_d}	23.26	22.67	25.05	28.37	38.32	46.61	63.23

Table 7 Rise time and peakings of ABESO for bandwidth changing from 5 to 7

Index	w_o								
	5			6			7		
e_i	e_x	$e_{\dot{x}}$	e_d	e_x	$e_{\dot{x}}$	e_d	e_x	$e_{\dot{x}}$	e_d
t_r	0.63	0.54	2.09	0.51	0.47	1.56	0.48	0.41	1.33
$|e_{max}|$	0.04	0.36	0.53	0.04	0.41	0.62	0.04	0.48	0.73

(a) e_1

(b) e_2

(c) e_3

(d) State

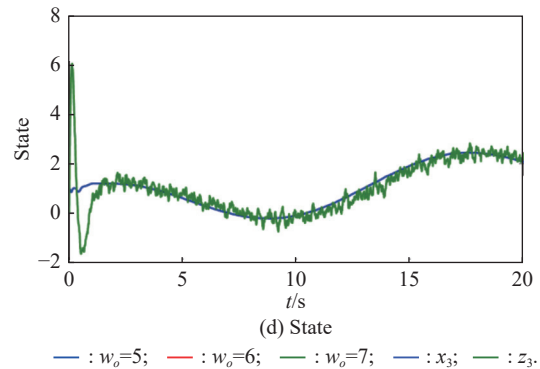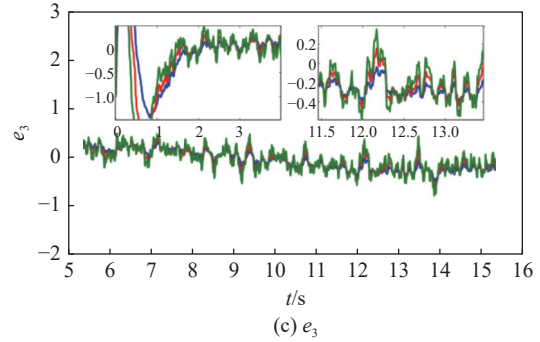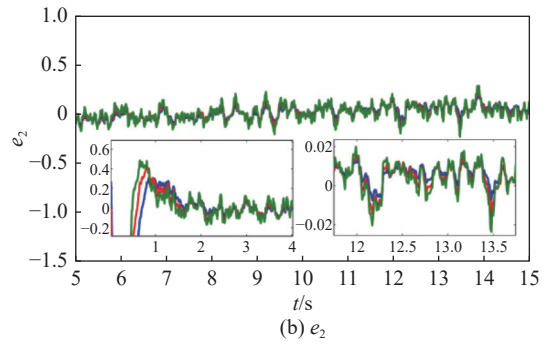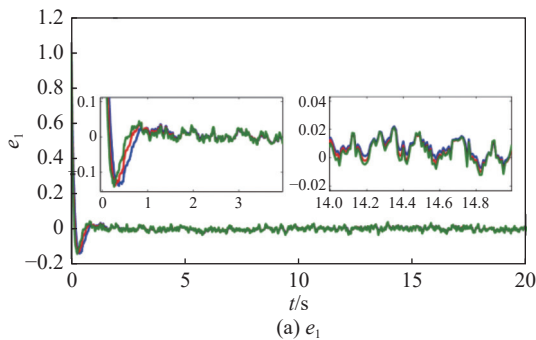—— : w_o=5; —— : w_o=6; —— : w_o=7; —— : x_3; —— : z_3.

Fig. 4 ABESO performances in estimating compound disturbances with measurement noise

Table 8 Comparison of performance indexes of ABESO and LESO with $w_o = 7$

Algorithm	Index					
	J_{e_x}	$J_{e_{\dot{x}}}$	J_{e_d}	$t_r(e_x)$	$t_r(e_{\dot{x}})$	$t_r(e_d)$
LESO	1.66	12.75	33.48	0.5	0.46	1.34
BESO	2.59	27.97	89.23	0.47	0.39	2.22
ABESO	1.57	11.03	28.37	0.48	0.41	1.33
Reduction[1]/%	4.89	13.46	15.28	4	10.87	0.75
Reduction[2]/%	39.26	60.56	68.21	-2.13	-5.13	40.09

5. Conclusions

In this paper, an extended state observer that switches the gain between two values is proposed to address disturbance and measurement noise in control systems.

ABESO is a 2-degree-of-freedom observer with two parameters to be designed, the gain and the bandwidth scaling factor, so that the bandwidth switches between w_o and $w_o\rho$. When the estimation error decreases, $\rho < 1$ can reduce the bandwidth to suppress the noise. It can be concluded that ABESO outperforms LESO and BESO in terms of state tracking and disturbance rejection when there is measurement noise. Rigorous convergence analysis and numerical simulations verify the effectiveness of the proposed method.

However, ABESO proposed in this paper has limitations. The design of extended state observer for a class of second-order nonlinear uncertain systems is studied. Although the gain switching strategy can be extended to higher-order systems, the stability analysis of higher-order switching systems is difficult. In addition, the gain of ABESO is switched according to the direction of the error, and the amplitude is fine-tuned on the basis of bandwidth. Although the sensitivity of the observer to noise is reduced, the effect on peaking value is not obvious. Using saturation nonlinearity to reduce the peaking value may be a solution. And we will investigate ESOs for higher-order systems with measurement noise in other ways.

References

[1] HAN J Q. From PID to active disturbance rejection control. IEEE Trans. on Industrial Electronics, 2009, 56(3): 900–906.

[2] SHI D, WU Z, CHOU W S. Generalized extended state observer based high precision attitude control of quadrotor vehicles subject to wind disturbance. IEEE Access, 2018, 6: 32349–32359.

[3] GRELEWICZ P, NOWAK P, CZECZOT J, et al. Increment count method and its PLC-based implementation for autotuning of reduced-order ADRC with smith predictor. IEEE Trans. on Industrial Electronics, 2021, 68(12): 12554–12564.

[4] TIAN J Y, ZHANG S F, YANG H B. Enhanced extended state observer based control for missile acceleration autopilot. ISA Transactions, 2020, 96: 143–154.

[5] SUN H, MADONSKI R, LI S H, et al. Composite control design for dystems with uncertainties and noise using combined extended state observer and kalman filter. IEEE Trans. on Industrial Electronics, 2022, 69(4): 4119–4128.

[6] ABDUL-ADHEEM W R, AZAR A T, IBRAHEEM K I, et al. Novel active disturbance rejection control based on nested linear extended state observers. Applied Sciences, 2020, 10(12): 4069.

[7] LAKOMY K, MADONSKI R. Cascade extended state observer for active disturbance rejection control applications under measurement noise. ISA Transactions, 2021, 109: 1–10.

[8] SUN L, ZHENG Z W. Disturbance-observer-based robust backstepping attitude stabilization of spacecraft under input saturation and measurement uncertainty. IEEE Trans. on Industrial Electronics, 2017, 64(10): 7994–8002.

[9] WANG H Y, ZUO Z Q, WANG Y J, et al. Composite nonlinear extended state observer and its application to unmanned ground vehicles. Control Engineering Practice, 2021, 109: 10734.

[10] XUE W C, ZHANG X C, SUN L, et al. Extended state filter based disturbance and uncertainty mitigation for nonlinear uncertain systems with application to fuel cell temperature control. IEEE Trans. on Industrial Electronics, 2020, 67(12): 10682–10692.

[11] BATTILOTTI S. Robust observer design under measurement noise with gain adaptation and saturated estimates. Automatica, 2017, 81: 75–86.

[12] AHRENS J H, KAALIL H K. High-gain observers in the presence of measurement noise: a switched-gain approach. Automatica, 2009, 45(4): 936–943.

[13] YANG L Y, LIU L L, ZHANG J. A bi-bandwidth extended state observer for a system with measurement noise and its application to aircraft with abrupt structural damage. Aerospace Science and Technology, 2021, 114: 106742.

[14] PRASOV A A, KHALIL H K. A nonlinear high-gain observer for systems with measurement noise in a feedback control framework. IEEE Trans. on Automatic Control, 2013, 58(3): 569–580.

[15] GAO Z Q. Scaling and bandwidth-parameterization based controller tuning. Proc. of the American Control Conference, 2003: 4989−4996.

[16] LIN H, ANTSAKLIS P J. Stability and stabilizability of switched linear systems: a survey of recent results. IEEE Trans. on Automatic Control, 2009, 54(2): 308–322.

Biographies

ZHANG Shihua was born in1981. She received her B.E. and M.E. degrees from Hebei Normal University, Shijiazhuang, China, in 2003 and 2006, respectively, and Ph.D. degree from the Army Engineering University of PLA, Shijiazhuang, China, in 2023. Her research interests include theory and application of active disturbance rejection control and flight control of unmanned aerial vehicle.
E-mail: zsh3991171@126.com

QI Xiaohui was born in1963. She received her B.E., M.E., and Ph.D. degrees from Nanjing University of Science and Technology, Nanjing, China, in 1983, 1988, 2010, respectively. She is a professor at the Department of Unmanned Aerial Vehicle Engineering, Army Engineering University of PLA. Her research interests include flight control theory and application or unmanned aerial vehicle, and adaptive control.
E-mail: qi-xh@163.com

YANG Sen was born in1984. He received his B.E. degree from Guilin University of Electronic Technology Guilin, China, in 2007, M.E. and Ph.D. degrees from the Department of Mechanical Engineering College, Shijiazhuang, China, in 2009 and 2013, respectively. He is a lecturer and the director at the Department of Unmanned Aerial Vehicle Engineering, Army Engineering University of PLA. His research interests include system parameter and identification and adaptive control.
E-mail: sanmu_oec@163.com